Proceedings of the 2011 6th IEEE International
Conference on Nano/Micro Engineered and Molecular Systems
February 20-23, 2011, Kaohsiung, Taiwan

Integration of Slanted Tether Check-valves for High Pressure Applications

Jeffrey Chun-Hui Lin*, *Student Member, IEEE*, Feiqiao Yu, Yu-Chong Tai, *Fellow, IEEE*
Electrical Engineering
California Institute of Technology
Pasadena, CA 91125, USA.
*Contacting Author: Jeffrey Chun-Hui Lin; E-mail: linch@mems.caltech.edu

Abstract—**We present a new approach to assemble multiple parylene check-valves to create a new device for high pressure microfluidic applications. By assembling several residual-stress-enhanced slanted tether check-valves in series, the cracking pressure of several psi can be easily achieved. The valve is modeled by extended valve theory considering the unsteady flow effect at the beginning of ckeck-covering plate's opening. A new equivalent diode model is also proposed to analyze and predict the check-valves' microfluidic behavior. Check-valves with thermally pre-stressed slanted tethers are chosen due to its remarkable high cracking pressure of each single check-valve. The slanted tethers are made using linearized partial exposure lithography technique and the tensile stress of the tethers is controlled by annealed in different temperatures. The size of each packaged single check-valve can be as small as 2 mm in length and 850 µm in diameter and the final packaged device with several integrated check-valves is capable of regulating pressure up to several psi. The testing result shows a higher cracking pressure with more check-valves, proving the series additivity of this model and integration. With its small size and high pressure regulating capability, the new check-valve system can be used to perform high pressure control application where the implantation space is limited. Different kind of parylene check-valves can also be combined to reach different pressure range using this packaging approach.**

Keywords-check-valve, microfluidic, parylene, lithography

I. INTRODUCTION

In the past, we have developed several kinds of check-valves with different cracking pressures depending on the device's applications [1-3]. Among all these check-valves, the slanted tether type is the one that can deliver the highest cracking pressure by quenching the valve to room temperature after a stress-relaxation annealing process to induce high residual tensile stress in the tethers as shown in Figure 1. However, even though the cracking pressure of this slanted tether check-valve can be adjusted by annealing at different temperature, the maximum cracking pressure achievable with a single valve is still limited by the bonding strength between parylene and silicon in the anchor region, and the ultimate tensile strength of the parylene tethers. To achieve even higher cracking pressures, we present the first demonstration that multiple slanted tether check-valves are used in series. In a series construction, each slanted tether check-valve could be modeled as a diode, where pressure and flow rate are analogous to voltage and current respectively. Using this model, multiple valves can be easily analyzed and connected in series to achieve a larger total pressure drop even though the pressure drop across each valve is smaller. This situation is similar to using a series connection of multiple diodes to achieve a higher total voltage drop.

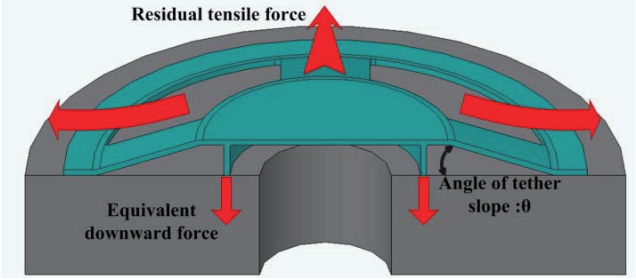

Figure 1. Pre-stressed, slanted-tether check-valve configuration. Annealing and then quenching is used to achieve a residual tensile force in the tethers.

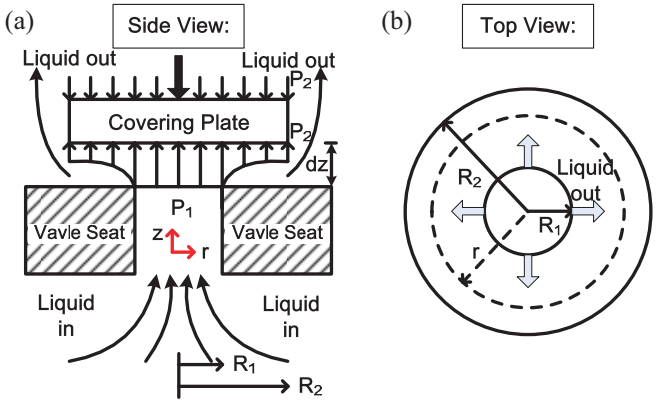

Figure 2. Valve model for unsteady flow analysis: (a) side view,and (b) top view.

II. DEVICE ANALYSIS AND DESIGN

A. Thin film flow theory of the check-valve

A simplified valve configuration is shown in Figure 2. The check-valve is normally closed at beginning owing to a pre-stressed downward force. The covering plate will open when the forwarding force of the liquid becomes higher than the downward force and then the liquid flows in between the covering plate and the valve seat, forming a very thin capillary flow layer. The flow rate in such case has not been fully developed so that the problem needs to take into account some unsteady flow effects. Several assumption are made to simplified the calculations: (1) The flow is incompressible, and

axisymmetrical; (2) the upstream pressure, p_1, is uniformly applied on the covering plate within the range of $r \le R_1$ and so is the downstream pressure, p_2, which is the pre-stressed downward force; (3) the weight of the liquid is negligible; (4) the opening gap, g, is much smaller than the R_1. At very low Reynolds number in this then film flow, the Navior-Stokes equation can be reduced into the Reynolds equations of hydrodynamic lubrication as follows [4]:

$$\frac{\partial p}{\partial z} = 0, and\ \frac{\partial p}{\partial r} = \mu \frac{\partial^2 u_r}{\partial z^2}, \tag{1}$$

where p is the pressure in the liquid film, μ is the dynamic viscosity and u_r is the radial velocity component. From integrating equation (1), we can get radial velocity as

$$u_r(z) = \frac{1}{2\mu}\frac{dp}{dr} z(z-g). \tag{2}$$

Therefore, the volume flow rate can be represented as

$$Q(r) = \int_0^g u_r(z) 2\pi r dz = -\frac{\pi}{6}\frac{r}{\mu}\frac{dp}{dr} g^3. \tag{3}$$

By conservation of mass, the volume flow rate can be also shown that

$$Q(r) = Q(R_1) - \pi\left(r^2 - {R_1}^2\right)\frac{dg}{dt}, \tag{4}$$

where $\pi\left(r^2 - {R_1}^2\right)\frac{dg}{dt}$ represents the volume increase within R_1 and r. Equal equations (3) and (4) yields

$$r\frac{dp}{dr} = \frac{6\mu}{g^3}\frac{dg}{dt}\left(r^2 - {R_1}^2\right) + R_1 \left(\frac{dp}{dr}\right)\Big|_{r=R_1}. \tag{5}$$

Let $\frac{r}{R_1} = \lambda\ and\ \frac{R_2}{R_1} = M$, and integrate equation (5) with respect to λ, then yields

$$p = \frac{3\mu}{g^3}\frac{dg}{dt}{R_1}^2(\lambda^2 - 2ln\lambda) + ln\lambda \left(\frac{dp}{d\lambda}\right)\Big|_{\lambda=1} + C. \tag{6}$$

To solve the constant C and $\left(\frac{dp}{d\lambda}\right)\Big|_{\lambda=1}$, substitute the boundary conditions $p=p_1$ at $\lambda=1$ and $p=p_2$ at $\lambda=M$ and we can get

$$C = p_1 - \frac{3\mu}{g^3}\frac{dg}{dt}{R_1}^2, \tag{7}$$

and

$$\left(\frac{dp}{d\lambda}\right)\Big|_{\lambda=1} = \frac{1}{lnM}\left[p_2 - p_1 + \frac{3\mu}{g^3}\frac{dg}{dt}{R_1}^2(1 - M^2 + 2lnM)\right]. \tag{8}$$

Substitute equation (7) and (8) into (6) and yields

$$\begin{aligned} p = p_2 + (p_1 - p_2)\left(1 - \frac{ln\lambda}{lnM}\right) \\ + \frac{3\mu}{g^3}\frac{dg}{dt}{R_1}^2\left[\lambda^2 - 1 + \frac{ln\lambda}{lnM}(1 - M^2)\right], \end{aligned} \tag{9}$$

and therefore, the volume flow rate of equation (3) becomes

$$Q(r) = (p_1 - p_2)\frac{\pi}{6\mu lnM} - \frac{\pi r}{2}\frac{dg}{dt}{R_1}^2\left(\frac{2r}{{R_1}^2} + \frac{1 - M^2}{rlnM}\right). \tag{10}$$

The total force that the liquid applied on the covering plate is

$$\begin{aligned} F_{Total} &= (p_1 - p_2)\pi{R_1}^2 + F_{plate} \\ &= (p_1 - p_2)\pi{R_1}^2 + \int_1^M p 2\pi\, {R_1}^2 \lambda d\lambda \\ &= \left[(p_1 - p_2)\pi{R_1}^2\left(\frac{M^2 - 1}{2lnM}\right)\right] \\ &\quad + \frac{\mu}{g^3}\frac{dg}{dt}\frac{3\pi}{2}{R_1}^4\left[1 - M^4 + \frac{1 - 2M^2 + M^4}{lnM}\right] \\ &= F_{steady} + F_{unsteady}, \end{aligned} \tag{11}$$

where F_{steady} represents the applied force in steady state flow due to $(p_1\text{-}p_2)$ while $F_{unsteady}$ represents the unsteady state condition. The second term becomes zero if the covering plate's gap is fixed, i.e. $\frac{dg}{dt} = 0$, or $R_1=R_2$, or the dynamic viscosity, μ, is zero.

B. Calculation of the necessary pre-stress force

The liquid starts flow when upstream force is equivalent or higher than the downstream force. The force balance at this moment can be used to find the necessary pre-stress tensile stress and can be represented as:

$$\begin{aligned} {p_1}\pi{R_1}^2 &\ge {p_2}\pi{R_2}^2 \\ \Rightarrow p_1 &\ge M^2 p_2 = p_c, \end{aligned} \tag{12}$$

where p_c is defined as the cracking pressure of the check-valve. Assume the tensile stress of the slanted tethers is σ_t, the tethers' number, thickness, width, and angle are n, t, w, and θ respectively, then the required tensile stress can be derived as

$$\sigma_t = \frac{\pi{R_1}^2}{twnsin\theta} p_c \tag{13}$$

where p_c is represented in equation (12). As the tensile stress is generated by annealing the check-valve in high temperature T_1 and quenched to room temperature T_r, σ_t can also be represented as

$$\sigma_t = E_p \alpha (T_1 - T_r), \tag{14}$$

where E_p and α is the Young's modulus and the thermal coefficient of expansion of parylene-C, respectively. So the annealing temperature can be determined by equation (14).

C. Electrical equivalent diode model

Consider the volume flow rate at $r=R_2$, which equals the final exit flow rate of the check-valve, this is calculated using equation (10) and can be rearranged as

$$\begin{aligned} Q(r)|_{r=R_2} &= (p_1 - p_2)\frac{\pi}{6\mu lnM} \\ &\quad - \frac{dg}{dt}\left(\pi{R_2}^2 + \frac{\pi}{2}\frac{{R_1}^2 - {R_2}^2}{lnM}\right). \end{aligned} \tag{15}$$

Therefore, in order to successfully generate the flow rate, the applying pressure of the liquid p_1 needs to be higher than the cracking pressure p_c shown in equation (12) and the flow rate is presented as in equation (15). The whole system can be equivalently modeled as a diode shown in Figure 3. with cut-in voltage as p_c. The flow rate in equation (15), can be modeled as the electrical current after the cut-in voltage.

D. Design of linearly slope sacrificial photoreist

The gray-scale partial exposed lithography technique is used here to create linearly slope sacrificial photoresist. An array of small dark squares, whose size smaller than the diffraction limit of the exposure apparatus, is utilized to make the photomask partially light transmittable as illustrated in Figure 4. The maximum square pitch size p, is expressed as

$$p \le p_c = \frac{1}{1+\sigma} \times \frac{\lambda'}{NA}, \tag{16}$$

where σ is the coherence factor of the optical system, λ' is the UV wavelength and NA is the numerical aperture of the exposure system [5]. Furthermore, since most photoresists have nonlinear response to UV light, a mathematical model is adopted to characterize and linearize the final photoresist profile [6]. According to the model, it can be shown that in

order to have a linear distribution of exposed photoresist, the dose of the exposure, $E(t)$ can be calculated as

$$E(t) = 1 - \exp(-\gamma I_0 T t), \quad (17)$$

where γ is the proportional constant, I_0 is the light intensity and T is the transmittance of the photomask, which can be derived by equation (17)

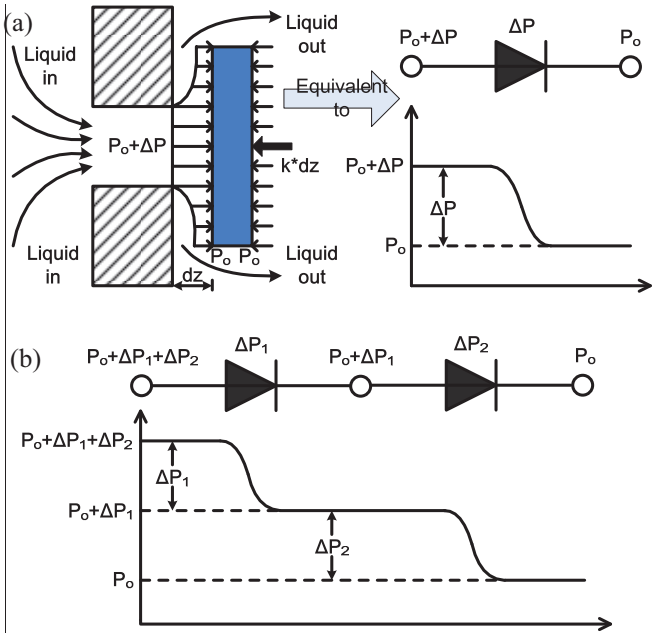

Figure 3. Equivalent electrical circuit component model of check-valves: (a) one diode model of one check-valve, (b) in series diodes model of in series check-valves. k and dz are the spring constant of the tethers and the covering plate displacement, respectively.

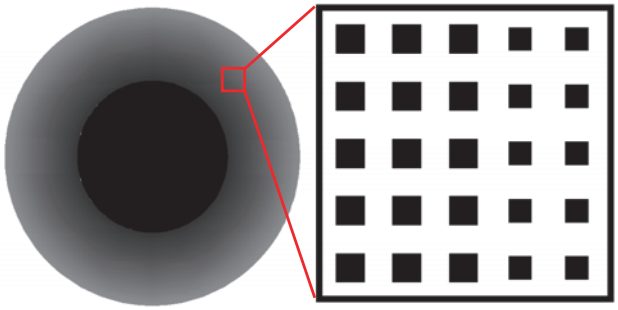

Figure 4. A closer view of gray-scale photomask for the creation of slanted photoresist. The right pattern shows the part of pixel structure of the ring.

III. Device Fabrication Procedures

The fabrication of each check-valve started with DRIE to pattern the valve's opening holes and releasing trench as shown in Figure 5. A 100 µm deep thin circular trench was etched on the front side followed by coating and patterning parylene as an anchor to help hold the parylene check-valve in place during valve operation. A layer of sacrificial photoresist with linear slopes was patterned using a grey scale photo mask. Then, a layer of 10 µm parylene-C was coated and patterned. After parylene patterning, the through hole was completed by DRIE, the sacrificial photoresist was removed, and the check-valves were released from the wafer. The results are show in Figure 6.

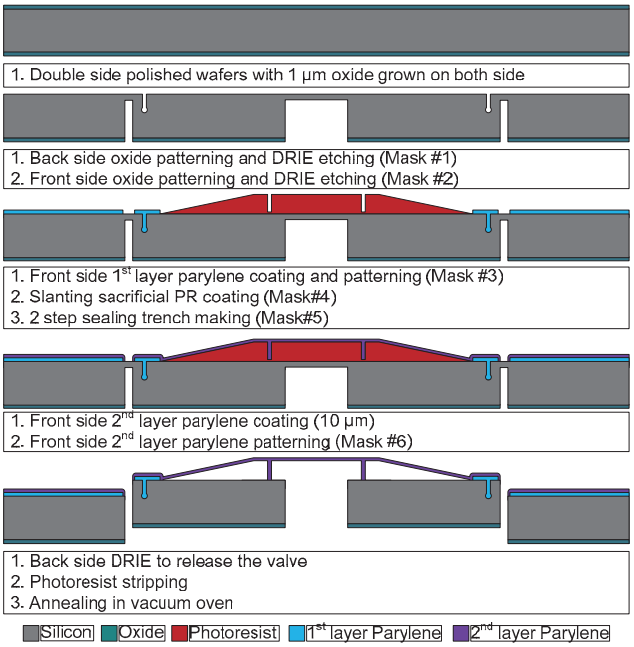

Figure 5. Fabrication procedures. Slanted photoresist is achieved using one-time exposure grey-scale photo mask photolithography approach.

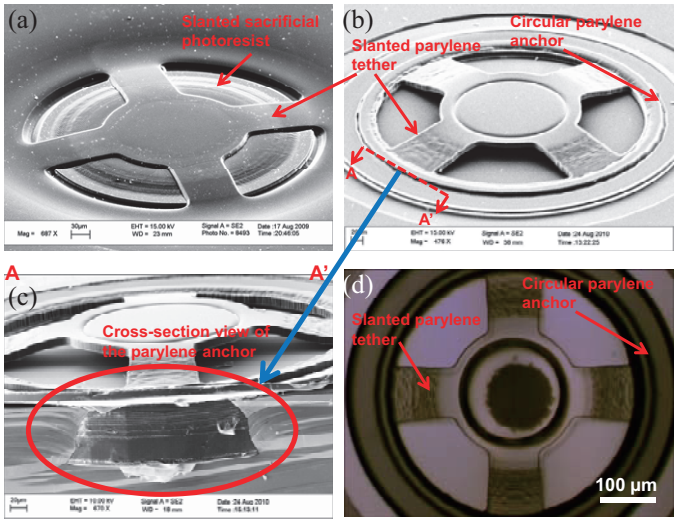

Figure 6. SEM pictures (a) before photoresist release, (b) after photoresist release, (c) cross-section view of the anchor, and (d) micrograph of the valve.

IV. Devices Integration, Testing and Conclusion

The check-valves were first annealed at 140ºC and then quenched to room temperature to indroduce the necessary residual tensile stress in tethers. To assemble the device, each check-valve was first inserted into a thin glass capillary tube, whose inner diameter is 530 µm, and sealed with epoxy as shown in Figure 7. These individual assemblies were then characterized to obtain their cracking pressure and flow profile. In this test, photoresist was used to seal the gap between the assembly and the Teflon tube so that the assembly can be released for further treatment (Figure 8.) Afterwards, each pair of assemblies were coupled together with a wider capillary tube (inner diameter of 660 µm), sealed with epoxy, and tested.

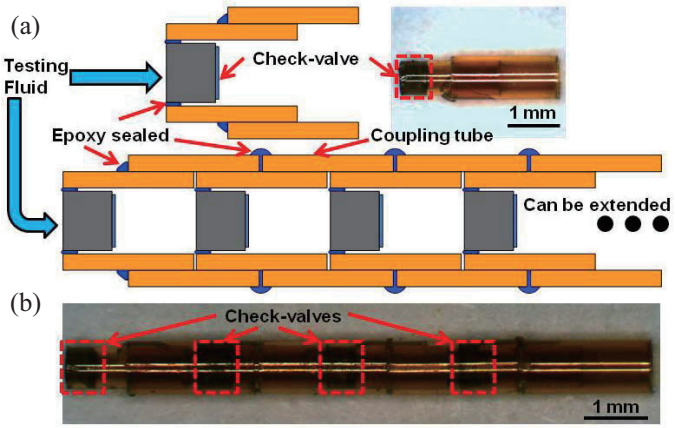

Figure 7. Valve packaging. (a) single valve packaged in capillary tubes and (b) 4 individual modules are integrated using coupling tubes.

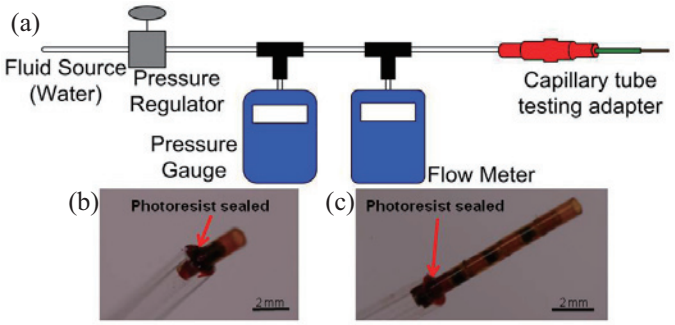

Figure 8. (a) Device testing setup, (b) a single valve, and (c) 4 valves in series.

The measured cracking pressures of each check-valve and the combined check-valve assembly are listed in Table I. the typical flow profiles of a single check-valve and of a 4 check-valve assembly are shown in Figure 9. The results show that the cracking pressure of a single valve falls between 0.42 psi and 0.49 psi but the overall cracking pressure is additive with more check-valves connected in series. For example, the cracking pressure rises up to 2.06 psi with 4 integrated check-valves were achieved. The parylene check-valves remain intact after many tests as shown in Figure 9.(b). This proves the durability of the parylene anchors, which are to prevent de-bonding due to both the high tensile stress within the parylene layer after annealing process and the high pressure during the entire testing process. The results verify the concept that integrating multiple slanted tether check-valves in series can create an additive cracking pressure device for microfluidic applications, and also proves the feasibility of pre-stress slanted tether check-valve's approach introducing residual tensile stress using thermal annealing and quenching.

TABLE I. MEASURED CRACKING PRESSURE

Single valve	1	2	3	4
Cracking Pressure	0.49 psi	0.43 psi	0.47 psi	0.42 psi
Multiple valves	**2 valves**	**3 valves**	**4 valves**	
Cracking Pressure	1.01 psi	1.48 psi	2.06 psi	

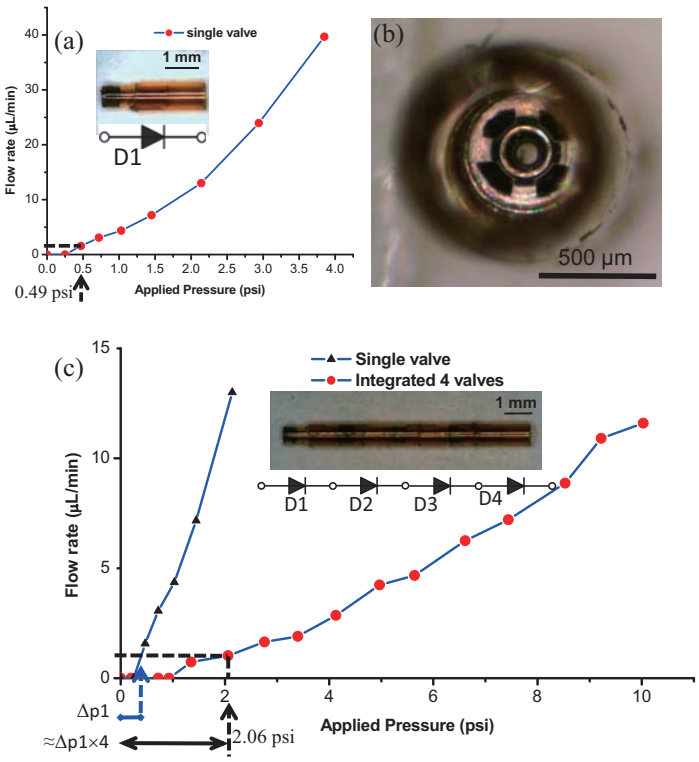

Figure 9. (a) flow characteristics of a single valve, (b) micrograph of valve in tube after testing. (c) flow characteristics of a 4-valve assembly.

ACKNOWLEDGEMENT

The authors would like to thank Trevor Ropers technical assistance in terms of device fabrication.

REFERENCES

[1] J. C.-H. Lin, P.-J. Chen, B. Yu, M. Humayun, Y-C. Tai, "Minimally Invasive Parylene Dual-Vavled Flow Drainage Shunt for Glaucoma Implant", in Tech. Digest 22nd IEEE International Conference on MicroElectroMechanical Systems (MEMS 2009), Sorrento, Italy, Jan. 25-29, pp.196-199.

[2] J. Lin, F. Yu, Y.-C. Tai, "Cracking Pressure Control of Parylene Check-valve Using Slanted Tensile Tethers," in Tech. Digest 23rd IEEE International Conference on MicroElectroMechanical Systems (MEMS 2010), Hongkong, Jan. 24-28, pp. 1107-1110.

[3] J. C.-H. Lin, P.-J. Chen, S. Saati, R. Varma, M. Humayun, Y.-C. Tai, "Implantable Microvalve-Packaged Glaucoma Drainage Tube", in Tech. Digest 13th Solid State Sens., Actuators, and Microsyst. Workshop, Hilton Head, SC, Jun. 1-5, 2008, pp. 146–149.

[4] R.A. Gabing, "Flow and Plate Motion in Comprssor Vavles", Ph.D. Thesis, University of Twente, The Netherlands, 2005.

[5] B. Wagner, H.J. Quenzer, W. Henke, W. Hoppe and W. Pilz, "Microfabrication of Complex surface Topographies Using Grey-tone Lithography," Sensors and Actuators A, 46-47, pp. 89-94, 1995.

[6] M. LeCompte, X. Gao and D. W. Prather, "Photoresist Characterization and Linearization Procedure for The Gray-Scale Fabrication of Diffractive Optical Elements" *Appl. Opt.*, Vol. 40, No. 32, pp.5921-5927, 2001.

[7] C. M. Waits, A. Modafe and Reza Ghodssi, "Investigation of Gray-scale Technology for Large Area 3D Silicon MEMS Structures," J. Micromech. Microeng. 13 pp. 170-177, 2003.

[8] M. Hu, H. Du, S.-F. Ling, Y. Fu, Q. Chen, L. Chow, B. Li, "A Silicon-on-Insulator Based Micro Check-valve", J. Micromech. Microeng., 14, pp. 382-387, 2004.